Published in final edited form as:
Mol Cancer Ther. 2009 March ; 8(3): 703–710. doi:10.1158/1535-7163.MCT-08-0656.

Molecular Imaging of Bcr-Abl Phosphokinase in a Xenograft Model*

Ji Yuan Wu[1], **David J. Yang**[2], **Laura S. Angelo**[1], **Saady Kohanim**[2], and **Razelle Kurzrock**[1]

1 *Department of Investigational Cancer Therapeutics (Phase I Program), Division of Cancer Medicine, The University of Texas M.D. Anderson Cancer Center, Houston, Texas*

2 *Department of Experimental Diagnostic Imaging, The University of Texas M.D. Anderson Cancer Center, Houston, Texas*

Abstract

The purpose of this study was to determine whether the Bcr-Abl tyrosine kinase can be assessed by gamma imaging using an ^{111}Indium-labeled anti-phosphotyrosine antibody, and if the response to treatment with imatinib could be detected using this imaging technique. Anti-phosphotyrosine antibody (APT) was labeled with indium (^{111}In) using ethylenedicysteine (EC) as a chelator. To determine if ^{111}In-EC-APT could assess a non-receptor tyrosine kinase, xenografts of the human chronic myelogenous leukemia (CML) cell line K562 were used. Gamma scintigraphy of the tumor-bearing mice, before and after imatinib treatment, was obtained 1, 24, and 48 hours after they were given ^{111}In-EC-APT (100 uCi/mouse, i.v.). ^{111}In-EC-APT is preferentially taken up by Bcr-Abl-bearing tumor cells when compared to ^{111}In-EC-BSA or ^{111}In-EC-IgG$_1$ controls, and comparable to the level of uptake of ^{111}In-EC-Bcr-Abl. Imatinib treatment resulted in decreased expression of phosphorylated Bcr-Abl by Western blot analysis, which correlated with early (four days after starting imatinib) kinase down-regulation as assessed by imaging using ^{111}In-EC-APT. The optimal time to imaging was 24 and 48 hours after injection of ^{111}In-EC-APT. Although tumor regression was insignificant on day 4 after starting imatinib treatment, it was marked by day 14. ^{111}In-EC-APT can assess intracellular phosphokinase activity, and down-regulation of phosphokinase activity predates tumor regression. This technique may therefore be useful in the clinic to detect the presence of phosphokinase activity, and for early prediction of response.

Keywords

^{111}In-EC-APT; CML; Bcr-Abl; anti-phosphotyrosine antibody; imatinib

INTRODUCTION

We are entering an age in which it may be feasible to use state-of-the-art imaging not only for the diagnosis of cancer and gauging the response to treatment, but also to determine which agents to use for therapy, and to predict the potential for response based on early target modulation. For example, positron emission tomography (PET) using 18-F-

*This publication was made possible by Grant Number RR024148 from the National Center for Research Resources (NCRR), a component of the National Institutes of Health (NIH), and NIH Roadmap for Medical Research.

Corresponding author: Razelle Kurzrock, MD, FACP, Professor of Medicine, Chair, Department of Investigational Cancer Therapeutics, [Phase I Clinical Trials Program], Division of Cancer Medicine, Anderson Clinical Faculty Chair for Cancer Treatment and Research, M. D. Anderson Cancer Center, Unit 455, P.O. Box 301402, Houston, TX 77030, Phone: 713-794-1226; Fax 713-563-0566, E-mail: rkurzroc@mdanderson.org.

fluorodeoxyglucose (18F-FDG) is widely used in clinical studies to identify metabolically active tumor cells. It is limited however by its non-specificity, i.e., it does not differentiate between types of tumors, nor at times between tumors and other inflammatory processes. Molecular imaging attempts to more specifically recognize protein targets, and one method of doing this exploits a homing agent bound to a radiotracer through a chelator, with the homing agent being a molecule that recognizes a protein specifically or preferentially expressed on cancer cells. Hence, imaging agents can be tailored to a specific malignancy based on the expression of cellular proteins, the availability of homing agents specific to that protein, and the availability of a chelator that can bind to the homing agent.

Recently, a few studies have begun to explore the possibility of receptor imaging using radio-labeled antibodies or bio-luminescence nanotechnology directed against the receptor, or with the use of labeled ligands that interact with the receptor, or with small molecule tracers (1–8). Such imaging technology has been applied to epidermal growth factor receptor (EGFR), Her2 receptor, vascular endothelial growth factor receptor (VEGFR), and TRAIL receptor in animal models (1–8). Apart from aberrant receptor tyrosine kinases, there are many other non-receptor tyrosine kinases, including src and Bcr-Abl, which when over-expressed or constitutively activated play a key role in the development of certain cancers. In addition, some of these tyrosine kinases are suppressed by small molecule inhibitors, such as imatinib or dasatinib or others, which target the ATP binding site in the tyrosine kinase domain (9–11). Indeed, there is a wealth of kinase inhibitors now entering clinical trials, and perhaps one of the most important questions in oncology today is how to predict which patients will respond to which kinase inhibitor. A non-invasive imaging technique that could detect the presence of the phosphorylated target and demonstrate early evidence of modulation by the drug administered would therefore be useful.

Antibodies are chosen for imaging studies based on the expression pattern of specific target molecules on the tumor cells. Following injection of radio-labeled antibodies, single photon emission computerized tomography (SPECT) images are taken at various time points to determine the optimal time to imaging after injection. This technique is noninvasive in contrast to biopsies, which contain sampling errors. Antibodies could also be used therapeutically if the antibody is linked to a radio-ablative molecule. The current study uses ^{111}In-labeled anti-phosphotyrosine antibodies to image the Bcr-Abl tyrosine kinase in a tumor-bearing xenograft. The specific uptake of radio-labeled antibody by the tumor and changes in imaging after treatment with imatinib were determined.

MATERIALS AND METHODS

Cell lines

K562 is a CML blast crisis cell line expressing constitutively activated Bcr-Abl tyrosine kinase. K562 was purchased from American Type Culture Collection (ATCC) (Rockville, MD). Cells were sub-cultured twice weekly in RPMI 1640 with 10% fetal bovine serum (Gemini-Bio-products, Woodland, CA), and maintained in a humidified incubator with 5% CO2.

Antibodies and reagents

Murine anti-phosphotyrosine antibody 4G10 was purchased from Upstate Biotechnology Incorporated (Charlottesville, VA) and used at a dilution factor of 1:2000. For Western blot analysis, murine anti-β-actin antibody was used as a control for protein loading (murine IgG_1, Sigma-Aldrich Company, St. Louis, MO). The anti-Abl, anti-Bcr-Abl antibody 8E9 is from BD Biosciences (San Jose, CA). Anti-phosphor-Bcr-Abl antibodies were obtained from Cell signaling Technology (Danvers, MA). The murine IgG_1 and anti-phosphor-Bcr-Abl antibodies were also used in the imaging portion of the study. Goat anti-rabbit or goat anti-

mouse IgG heavy and light chain secondary antibody was purchased from BioRad Laboratories (Hercules, CA). PEG-300 was purchased from Sigma- Aldrich (St Louis, MO), and imatinib was purchased from Novartis, Inc. (Cambridge, MA).

Western blot analysis

Western analysis was used to detect steady-state levels of phosphorlyated Bcr-Abl proteins. Cells were collected, washed once with PBS, and lysed in solubilization buffer (40 mM HEPES, PH 7.4, 150 mM NaCl, 1.5 mM $MgCl_2$, 1 mM EGTA, 1mM EDTA, 100mM NaF, 10mM sodium pyrophosphate, 10% glycerol, 1% Triton X-100, plus protease inhibitors: 1 mM PMSF, 1mM sodium vanadate, 10ug/ml leupeptin, and 10ug/ml aprotinin) for 30 minutes on ice. Total cell lysates were obtained after centrifugation at 14,000 RPM for 5 minutes. Protein concentration was measured using the BCA kit (Pierce Biotechnology, Rockford, IL), and 20 μg protein per lane was loaded onto an 8% SDS-PAGE gel. Proteins were transferred to nitrocellulose. The membrane was blocked with 3% bovine serum albumin (BSA) in Tris-buffered saline (TBS) containing 0.1% tween-20 for 1 hour, and then incubated with primary antibody in 3% BSA at room temperature for two hours, or at 4°C overnight. Blots were washed, and then incubated with either goat anti-rabbit secondary antibody (1:3,000) or goat anti-mouse secondary antibody (1:4,000) (BioRad Laboratories, Hercules, CA) for one hour and detected by enhanced chemiluminescence (ECL) (Amersham Pharmacia Biotech, Piscataway, NJ). Blots were exposed to film (Kodak Biomax).

Preparation of ^{111}In-EC –phosphotyrosine antibody

The antibodies were labeled with ^{111}Indium (^{111}In, t1/2= 2.805 days). ^{111}In isotope was selected to allow for a longer time observation. Ethylenedicysteine (EC) was selected as a chelator because EC-drug conjugates can be labeled with ^{111}In easily and efficiently with high radiochemical purity and stability (12–14). Synthesis of EC was prepared in a two-step manner as described (15,16). EC was conjugated to either anti-phosphotyrosine antibody, murine IgG_1, anti-phosphor-Bcr-Abl, or bovine serum albumin (BSA) using sulfo-N-hydroxysuccinimide and 1-ethyl-3-(3-dimethylaminopropyl) carbodiimide HCl as coupling agents. BSA was stirred with EC, sulfo-N-hydroxysuccinimide, and 1-ethyl-3-(3-dimethylaminopropyl) carbodiimide HCl at room temperature for 17 hours. After dialysis, 2.3 to 3.4 mg of EC antibody was obtained. The ^{111}Indium was added into a vial containing EC antibody (0.1 mg) to yield ^{111}In-EC-BSA, ^{111}In-EC-IgG_1, ^{111}In–EC-Bcr-Abl, or ^{111}In-EC-APT. Radiochemical purity for EC antibodies (Rf = 0.1) were >95% as determined by radio-TLC (Bioscan, Washington, DC) and labeled antibodies were eluted with saline or acetone.

Growth of K562 tumors in immuno-deficient mice

All animal work was approved by the University of Texas M.D. Anderson Institutional Animal Care and Use Committee. Six week-old female Swiss nude mice were provided by the Department of Experimental Radiology (M.D. Anderson Cancer Center, Houston, TX). Mice were housed in sterile filter-capped micro-isolator cages and provided with sterilized food and water. 6×10^6 K562 cells/100 μl/mouse were mixed with 50% matrigel (BD Biosciences San Jose, CA) in RPMI 1640 and injected subcutaneously into the right rear flank of the mouse. For the K562 tumor growth curve, a total of ten mice were divided into two groups: a control group given vehicle alone and a group treated with imatinib. In the control group, 100 μl of PEG-300 resuspended in sterile water was given by oral gavage; imatinib (100mg/kg) was given to the mice in the experimental group in the same manner as the vehicle control was delivered. Treatment was initiated when the tumors were 0.3 cm in size. Body weight and tumor size were measured every other day until day 14 after treatment. Tumor size or volume was calculated as $V= (L \times W^2) \times 0.52$, where L is the length and W is the width of the xenograft.

Mice were sacrificed and tumors were removed and minced. K562 tumor cells were lysed and the phosphorylation status of Bcr-Abl was assessed for both treatment and control groups.

Imaging of K562 (Bcr-Abl-positive) tumors in immuno-deficient mice

K562 tumor-bearing mice were divided into three groups for the imaging portion of the study. Group I received ^{111}In-EC-BSA (n=5). Group II received ^{111}In-EC-anti-phosphotyrosine (APT) (n=5). Group III also received ^{111}In-EC-anti-phosphotyrosine monoclonal antibody (APT) (n=5). Mice in Groups I and II did not receive imatinib treatment. Mice in Group III were treated with imatinib (100mg/kg daily). Two additional groups of five mice were injected with either ^{111}In-EC-IgG$_1$ or ^{111}In-EC-Bcr-Abl antibody as negative and positive controls, respectively. The imaging portion of the study was initiated three days after the start of treatment. 100μCi of ^{111} Indium labeled compound (^{111}In-EC-BSA, ^{111}In-EC-IgG$_1$, ^{111}In-EC-Bcr-Abl, or ^{111}In-EC-APT) was injected through the tail vein. Imatinib treatment in group III continued throughout the imaging process. Scintigraphic images were acquired at 1, 2, 24, or 48 hours following radiotracer injection using a gamma camera (M-camera, Siemens Corporation, New York, NY) equipped with a medium energy collimator. This camera provides planar images. Regions of interest (counts per pixel) at the tumor lesion site and the symmetrical normal muscle site were used to determine tumor/muscle count density ratios. The ratios were used to compare the dynamic changes in the phosphorylation state of Bcr-Abl in the cytoplasm after imatinib treatment, and also as a reflection of the uptake of labeled antibody by the cells (significance determined by student's t test). To verify tumor size and phosphorylation status precisely, one mouse from each group was selected for SPECT-CT (single photon emission computerized tomography) (Gammar Medica Corporation, Northridge, CA). The mice were anesthetized by inhalation of isofluorine with oxygen and scanned by CT first with 512 slides, then SPECT-CT with 32 frames. All the images were finally fused together using the Amira software (Mercury Computer Systems, Inc., Chelmford, MA) for bony structures or the Amide software (Crump Institute for Molecular Imaging, UCLA School of Medicine, California) for soft tissue analysis.

RESULTS

^{111}In-labeled anti-phosphotyrosine antibodies are exploitable for imaging Bcr-Abl-positive xenografts

To determine whether anti-phosphotyrosine antibodies can be exploited for assessing non-receptor tyrosine kinase Bcr-Abl positive tumors, K562 xenografts were injected with ^{111}In-labeled BSA (bovine serum albumin) or ^{111}In-labeled anti-phosphotyrosine antibody (APT). BSA serves as a marker of blood flow to the tumor. Thus, normal blood flow to the tumor versus specific uptake of ^{111}In-EC-APT can be visualized. Ethylenedicysteine (EC) was selected as a chelator for all radiotracers employed in this study. Nude mice were injected with K562 tumor cells and the tumors were allowed to grow to 0.3 cm in diameter. Mice in the imatinib treated group began therapy three days prior to the injection of ^{111}In-labeled antibodies and continued treatment during antibody injection for a total of 4 or 5 days of treatment for the imaging portion of the study. SPECT-CT (single photon emission computerized tomography) images acquired 48 hours after injection of ^{111}In-EC-BSA or ^{111}In-EC-APT are shown in Figure 1. The tumor is indicated by arrows. Injection of ^{111}In-EC-APT antibody results in increased tumor uptake compared to injection of control ^{111}In-EC-BSA as determined by enhanced tumor-to-non-tumor count density ratios (see supplemental data for three dimensional movie file).

To verify tumor size and phosphorylation status precisely, one mouse from each group was selected for SPECT-CT. Images were fused together using the Amira software, which allows visualization of bony structures in three dimensions (Figure 1.). SPECT-CT is a dynamic

imaging process that combines functional and structural elements. Thus, SPECT-CT shows the structure of the organism, the location of the tumor, and also detects the radioactive density of a specific area using computer software to enhance the image. Treatment with imatinib resulted in decreased uptake by the tumor of ^{111}In-EC-APT (Figure 1.). Coronal SPECT-CT was also used to visualize the amount of ^{111}In-EC-APT taken up by the tumor (Figure 2.). The difference between these images and the ones showing the bony structure (Figure 1.) is the software used to analyze the image. The Amide software was used to analyze soft tissue uptake of the radiotracer in the coronal images (Figure 2.). The tumor is indicated by arrows. ^{111}In-EC-APT injected mice show increased signal from the tumor as compared to ^{111}In-EC-BSA injected mice. Mice treated with imatinib for a total of five days exhibit decreased tumor signal (Figure 2).

Unlike SPECT-CT, planar imaging is static and two-dimensional. Planar images are taken on a flat surface, and can be used to measure the uptake of radio-labeled antibodies by the tumor in comparison to normal surrounding tissue. Regions of interest (counts per pixel) at the tumor lesion site and the symmetrical normal muscle site were used to determine tumor/muscle count density ratios. Scintigraphic images were taken 2, 24, or 48 hours following radio-labeled antibody injection. A comparison of the uptake of all radio-labeled compounds is shown in Figure 3a. K562 xenografts were injected with ^{111}In-EC-BSA, ^{111}In-EC-IgG$_1$, ^{111}In-EC-APT, or ^{111}In-EC-Bcr-Abl. Indium-labeled IgG$_1$ and BSA were used as negative controls, while ^{111}In-EC-Bcr-Abl was used as a positive control. Both negative control molecules had decreased T/M ratios when compared to either ^{111}In-EC-APT or ^{111}In-EC-Bcr-Abl (T/M: BSA= 1.5, IgG$_1$= 1.9, APT= 4.0, Bcr-Abl= 6.0) at the 48 hour time point when uptake was the greatest (Figure 3a and 3b).

Imatinib treatment of K562 (Bcr-Abl-positive) xenografts results in decreased tumor volume and decreased expression of phosphorylated Bcr-Abl by Western blot analysis

The effect of imatinib on K562 tumor growth was determined by calculating the tumor volume for mice treated with vehicle (PEG 300) or imatinib (100 mg/kg). For the K562 tumor growth curve, a total of ten mice were divided into two groups: a control group given vehicle alone and a group treated with imatinib. In the control group, 100 μl of vehicle resuspended in sterile water was given by oral gavage daily. Imatinib (100mg/kg) was given to the mice in the experimental group in the same manner as the vehicle control was delivered. Body weight and tumor size were measured every other day until day 14 after treatment. An increase (235%) in tumor volume was seen in the mice treated with vehicle (top) when compared to the mice treated with imatinib (87% decrease) (bottom) over the same 14 day period (Figure 4a.).

Levels of phosphorylated Bcr-Abl were analyzed by Western blot analysis to verify the anti-kinase effect of imatinib on Bcr-Abl in the xenografts. After tumor growth reached 0.3 cm, vehicle or imatinib was administered to the mice for 14 days. Mice were sacrificed and tumors were removed and minced. Cells were lysed and the phosphorylation status of Bcr-Abl was assessed for both treatment and control groups by Western blot analysis (Figure 4b.). Three different pairs of mice were analyzed for the expression of phospho-Bcr-Abl and phospho-Abl in the presence or absence of imatinib. Phospho-Bcr-Abl and phospho-Abl levels are decreased following treatment with imatinib for 14 days in each of the xenografts studied. Total levels of Bcr-Abl and Abl protein remain unchanged following imatinib treatment. The K562 cell line was used as a positive control for the effect of imatinib (data not shown), and β-actin was used as a loading control (Figure 4b.).

Planar imaging shows a higher tumor/muscle ratio for ^{111}In-EC-APT and a decrease in tumor uptake of radio-labeled antibody following treatment with imatinib at 24 and 48 hrs post injection

Scintigraphic images were taken 24 or 48 hours following radio-labeled antibody injection. Tumor/muscle count density ratios were used to compare the dynamic changes in the phosphorylation state of Bcr-Abl in the cytoplasm after imatinib treatment, and also as a reflection of the uptake of labeled antibody by the cells. Mice in the imatinib treated group began therapy three days prior to the injection of ^{111}In-EC-APT and continued treatment during antibody injection for a total of either 4 days (24 hr imaging) or 5 days (48 hr imaging) of treatment. Representative scintigraphic imaging of ^{111}In-labeled compounds in K562 xenografts are shown in Figure 5a. The computer outlined region of interest shows higher tumor/muscle ratios as a function of time in ^{111}In-EC-APT injected mice as compared to ^{111}In-EC-BSA injected mice (Figure 5a and 5b.). Decreased tumor/muscle ratios were detected by scintigraphic imaging in the imatinib treated mice at 24 and 48 hours post injection (Figure 5b., $p<0.05$). Mice treated with vehicle alone showed no decrease in Bcr-Abl phosphorylation by scintigraphic imaging (data not shown). Images were also taken at one hour post injection, but uptake of radio-labeled antibodies was not evident at this time (data not shown). These results indicate that ^{111}In-EC-APT antibodies are preferentially taken up by the tumor cells, and also that intracellular tyrosine kinases can be visualized with anti-phosphotyrosine antibodies, and the response to imatinib can be visualized within 4 days of the start of treatment.

DISCUSSION

Although kinase inhibitor treatment is proving successful in the clinic, the greatest challenge lies in predicting which patients will respond to this therapy. Traditional techniques used to predict patient responses to therapy include biopsies, which are invasive, painful, and potentially dangerous. In addition, data obtained from biopsies vary within the same patient and can therefore be unreliable. The development of novel imaging agents and techniques that would facilitate the prediction of responses to therapy is of paramount importance. The imaging technique presented here is potentially applicable to the clinic in that our experiments suggest that it allows assessment of the expression of the target molecule (constitutively phosphorylated tyrosine residues), and the effect of the kinase inhibitor on the target, in an animal model.

SPECT-CT provides target-specific cellular-based imaging findings. Other techniques used to monitor response include fluorescent in situ hybridization (FISH), quantitative polymerase chain reaction (PCR) for Bcr-Abl, and the assessment of phosphorylated CrkL. These techniques are valuable, but may be limited by sampling errors. SPECT-CT images provide real-time dynamic macroscopic whole-body bio-distribution of a radiolabeled antibody. It can accurately quantify the tumor volume via CT attenuation correction. SPECT-CT, while expensive when compared to other methods of Bcr-Abl assessment offers the advantage of seeing the result of treatment at an earlier stage (western blot = 14 days for inhibition of Bcr-Abl; tumor volume = 14 days; imaging = 4 days), and can help predict for response by measuring levels of kinase activity prior to treatment. Also, it offers a non-invasive way to assess the effectiveness of treatment.

Previous studies by our group using anti-epidermal growth factor receptor (EGFR) antibody (C225), anti-TRAIL death receptor 4 and 5 (DR4 and DR5) antibodies, and anti-17β-estradiol antibodies demonstrate the potential for these novel imaging techniques to detect their targets (1,8,17). In addition, our group has shown that anti-phosphotyrosine antibody detects the phosphorylation of frequently over-expressed or constitutively activated tyrosine kinase receptors such as EGFR. These antibodies can identify which tumors bear the target molecule,

and demonstrate early EGFR phosphokinase down-regulation before that predicted for tumor response *in vivo* using a mouse model (Gong et al., manuscript submitted).

The present study examines the potential use of radio-labeled anti-phosphotyrosine antibodies to image tumors over-expressing an intracellular phosphotyrosine molecule. To our knowledge, this is the first use of an anti-phosphotyrosine antibody to visualize an intracellular (non-receptor) kinase phosphorylated on tyrosine, and to successfully image the tumor after treatment with the kinase inhibitor imatinib.

The mechanism of entry of ^{111}In-EC-APT into the cell is dependent on the cellular target and the chelator. Ethylenedicysteine (EC) is the most recent and successful example of N_2S_2 chelates (18–21). EC can be labeled with metallic isotopes easily and efficiently with high radiochemical purity and stability (12–14). Certain antibodies (e.g. anti-EGFR and anti-CEA) bind to antigen and can be internalized through the endocytotic process (22–24). Endocytosis occurs either through specific enzymatic involvement or specific protein domains. Our biodistribution studies show internalization of the anti-phosphotyrosine antibody. This internalization might be due to antigen-antibody mediated induction of translocated protein following attachment to the host cell at the site of entry, and is associated with the endocytotic process. Additionally, K562 cells express the FcγRIIa receptor exclusively (25), which binds to all IgG subclasses. This Fc receptor may contribute to radio-labeled antibody uptake; however, antigen specificity may be more important as evidenced by the high T/M ratios seen in ^{111}In-EC-Bcr-Abl injected xenografts. Further study is warranted to evaluate which domain of the anti-phosphotyrosine antibody is required for endocytosis. We have used this strategy previously to successfully image angiogenesis by EC-endostatin (26), EGFR (1,27), apoptosis by EC-annexin V (20), and TRAIL (death) receptor by EC-ETR1 and EC-ETR2 antibodies (8).

Chronic myelogenous leukemia (CML) is a myeloproliferative disorder, whose dominant oncogenic product is the Bcr-Abl non-receptor tyrosine kinase. Bcr-Abl resides in the cytoplasm and drives CML and Philadelphia chromosome positive acute lymphocytic leukemia (ALL) growth (9). Targeting Bcr-Abl kinase activity results in dramatic responses in the clinic (10,11). Although CML is not typically a solid tumor, chloromas are extramedullary tumor nodules that can occur in this type of leukemia (28). It is conceivable that chloromas could be visualized by this technique. The transduction-transplantation model of CML could also be explored in the future to more thoroughly investigate the use of this technique in CML (29). More importantly, our model demonstrates the potential for our imaging technique to detect an intracellular kinase. Many oncogenic kinases are intracellular and since even receptor kinases are phosphorylated on their intracellular domains, our results support the potential for such imaging to be applied in the clinical setting.

Our experiments demonstrated that down-regulation of Bcr-Abl kinase could be demonstrated by imaging after only four days of treatment with imatinib (Figure 5a.), a point at which there is negligible change in growth (Figure 4a.). While tyrosine kinases other than Bcr-Abl would be detected by our imaging antibody, it is known that the predominant phosphokinase down-regulated by imatinib in K562 CML cells is Bcr-Abl, and this is consistent with our Western blot data (Figure 4b.). Clear regression of tumor occurred later (Figure 4a.). Therefore, the imaging results were able to predict tumor response. Although cell death may account for some of the shutdown in kinase imaging, it is unlikely to account for the dramatic results seen so early after imatinib treatment, especially in light of lack of tumor regression at that point. Hence, it is worthwhile to study the ability of imaging agents such as ^{111}In-EC-APT to detect baseline levels of phosphokinase in patients, and also for the initial selection of a specific kinase inhibitor as treatment. The latter could be accomplished by using specific anti-phosphotyrosine antibody-based imaging agents such as anti-phospho-kit or anti-phospho-EGFR to establish

the presence of the target kinase before treatment with a kit or EGFR kinase inhibitor, respectively. Furthermore, detection of kinase down-regulation after only a few days of therapy could be studied as a potential early predictor of response in the clinical setting.

Abbreviations

EC
: Ethylenedicysteine

^{111}In
: Indium

APT
: anti-phosphotyrosine

Bcr-Abl
: breakpoint cluster region-Abelson leukemia virus

References

1. Schechter NR, Yang DJ, Azhdarinia A, et al. Assessment of EGF receptors with ^{99m}Tc ethylenedicysteine-C225 monoclonal antibody. Anti-Cancer Drugs 2003;14:49–56. [PubMed: 12544258]
2. Kramer-Marek G, Kiesewetter DO, Martiniova L, Jagoda E, Lee SB, Capala J. [(18)F]FBEM-Z (HER2:342)-Affibody molecule-a new molecular tracer for in vivo monitoring of HER2 expression by positron emission tomography. Eur J Nucl Med Mol Imaging 2008;35:1008–18. [PubMed: 18157531]
3. Takahashi N, Yang DJ, Kohanim S, et al. Targeted functional imaging of estrogen receptors with ^{99m}Tc-GAP-EDL. Eur J Nucl Med Mol Imaging 2007;34:354–62. [PubMed: 17021817]
4. Cai W, Niu G, Chen X. Multimodality imaging of the HER-kinase axis in cancer. Eur J Nucl Med Mol Imaging 2008;35:186–208. [PubMed: 17846765]
5. Welsher K, Liu Z, Daranciang D, Dai H. Selective probing and imaging of cells with single walled carbon nanotubes as near-infrared fluorescent molecules. Nano Lett 2008;8:586–90. [PubMed: 18197719]
6. Cai W, Chen X. Multimodality imaging of vascular endothelial growth factor and vascular endothelial growth factor receptor expression. Front Biosci 2007;12:4267–79. [PubMed: 17485373]
7. Pai A, Giekas A, Doubrovin M, et al. Molecular imaging of EGFR kinase activity in tumors with ^{124}I-labeled small molecular tracer and positron emission tomography. Mol Imaging Biol 2006;8:262–77. [PubMed: 16897320]
8. Gong J, Yang DJ, Kohanim S, Humphreys R, Broemeling L, Kurzrock R. Novel in vivo imaging shows up-regulation of death receptors by paclitaxel and correlates with enhanced antitumor effects of receptor agonist antibodies. Mol Cancer Ther 2006;5:2991–3000. [PubMed: 17148761]
9. Kurzrock R, Shtalrid M, Romero P, et al. c-abl protein product in Philadelphia-positive acute lymphoblastic leukaemia. Nature 1987;325:631–5. [PubMed: 3543692]
10. Talpaz M, Shah NP, Kantarjian H, et al. Dasatinib in imatinib-resistant Philadelphia chromosome-positive leukemias. N Engl J Med 2006;354:2531–41. [PubMed: 16775234]
11. Druker BJ, Sawyers CL, Kantarjian H, Resta DJ, Reese SF, Ford JM, et al. Activity of a specific inhibitor of the BCR-ABL tyrosine kinase in the blast crisis of chronic myeloid leukemia and acute lymphoblastic leukemia with the Philadelphia chromosome. N Engl J Med 2001;344:1038–42. [PubMed: 11287973]
12. Blondeau P, Berse C, Gravel D. Dimerization of an intermediate during the sodium in liquid ammonia reduction of l-thiazolidine-4-carboxylic acid. Can J Chem 1967;45:49–52.
13. Van Nerom CG, Bormans GM, De Roo MJ, Verbruggen AM. First experience in healthy volunteers with Tc-99m-L-ethylenedicysteine, a new renal imaging agent. Eur J Nucl Med 1993;20:738–46. [PubMed: 8223766]

14. Surma MJ, Wiewiora J, Liniecki J. Usefulness of Tc-99m-N, N′-ethylene-1- dicysteine complex for dynamic kidney investigations. Nucl Med Commun 1994;15:628–35. [PubMed: 7970444]
15. Ilgan S, Yang DJ, Higuchi T, et al. ^{99m}Tc-ethylenedicysteine-folate: a new tumor imaging agent: synthesis, labeling, and evaluation in animals. Cancer Biother Radiopharm 1998;13:427–35. [PubMed: 10851435]
16. Zareneyrizi F, Yang DJ, Oh CS, et al. Synthesis of ^{99m}Tc ethylenedicysteine colchicine for evaluation of anti-angiogenic effect. Anti-cancer Drugs 1999;10:685–92. [PubMed: 10507319]
17. Takahashi N, Yang DJ, Kurihara H, et al. Functional imaging of estrogen receptors with radiolabeled-GAP-EDL in rabbit endometriosis model. Acad Radiol 2007;14:1050–7. [PubMed: 17707312]
18. Yang D, Yukihiro M, Yu DF, et al. Assessment of therapeutic tumor response using ^{99m}Tc-ethylenedicysteine-glucosamine. Cancer Biother and Radiopharm 2004;19:443–456.
19. Yang DJ, Kim C-G, Schechter NR, et al. Imaging with ^{99m}Tc-EC-DG targeted at the multifunctional glucose transport system: feasibility study with rodents. Radiology 2003;226:465–73. [PubMed: 12563141]
20. Yang DJ, Azhdarinia A, Wu P, et al. In vivo and in vitro measurement of apoptosis in breast cancer cells using ^{99m}Tc-EC- Annexin V. Cancer Biotherapy and Radiopharmaceuticals 2001;16:73–83. [PubMed: 11279800]
21. Yang DJ, Ozaki K, Oh CS, et al. ^{99m}Tc-EC-Guanine:synthesis, bio-distribution, and tumor imaging in animals. Pharmaceutical Research 2005;22:1471–9. [PubMed: 16132359]
22. Perera RM, Zoncu R, Johns TG, et al. Internalization, intracellular trafficking, and biodistribution of monoclonal antibody 806: a novel anti-epidermal growth factor receptor antibody. Neoplasia 2007;9:1099–110. [PubMed: 18084617]
23. Schmidt MM, Thurber GM, Wittrup KD. Kinetics of anti-carcinoembryonic antigen antibody internalization: effects of affinity, bivalency, and stability. Cancer Immunol Immunother. 2008 Apr 12;Epub ahead of print
24. Avignolo C, Bagnasco L, Biasotti B, et al. Internalization via Antennapedia protein transduction domain of an scFv antibody toward c-Myc protein. FASEB J 2008;22:1237–45. [PubMed: 18048579]
25. Allhorn M, Olin AI, Nimmerjahn F, Collin M. Human IgG/FccR Interactions Are Modulated by Streptococcal IgG Glycan Hydrolysis. PLoS ONE 2008;3:e1413. [PubMed: 18183294]
26. Yang DJ, Kim KD, Schechter NR, et al. Assessment of anti-angiogenic effect using ^{99m}Tc-EC-endostatin. Cancer Biother Radiopharm 2002;17:233–45. [PubMed: 12030117]
27. Schechter NR, Wendt RE 3rd, Yang DJ, et al. Radiation dosimetry of ^{99m}Tc-labeled C225 in patients with squamous cell carcinoma of the head and neck. J Nucl Med 2004;45:1683–7. [PubMed: 15471833]
28. Fritz J, Vogel W, Bares R, Horger M. Radiologic spectrum of extramedullary relapse of myelogenous leukemia in adults. AJR Am J Roentgenol 2007;189:209–18. [PubMed: 17579173]
29. Cuiffo B, Ren R. Models of hematopoietic malignancies: chronic myeloid leukemia. Drug Discovery Today: Disease Models 2006;3:183–9.

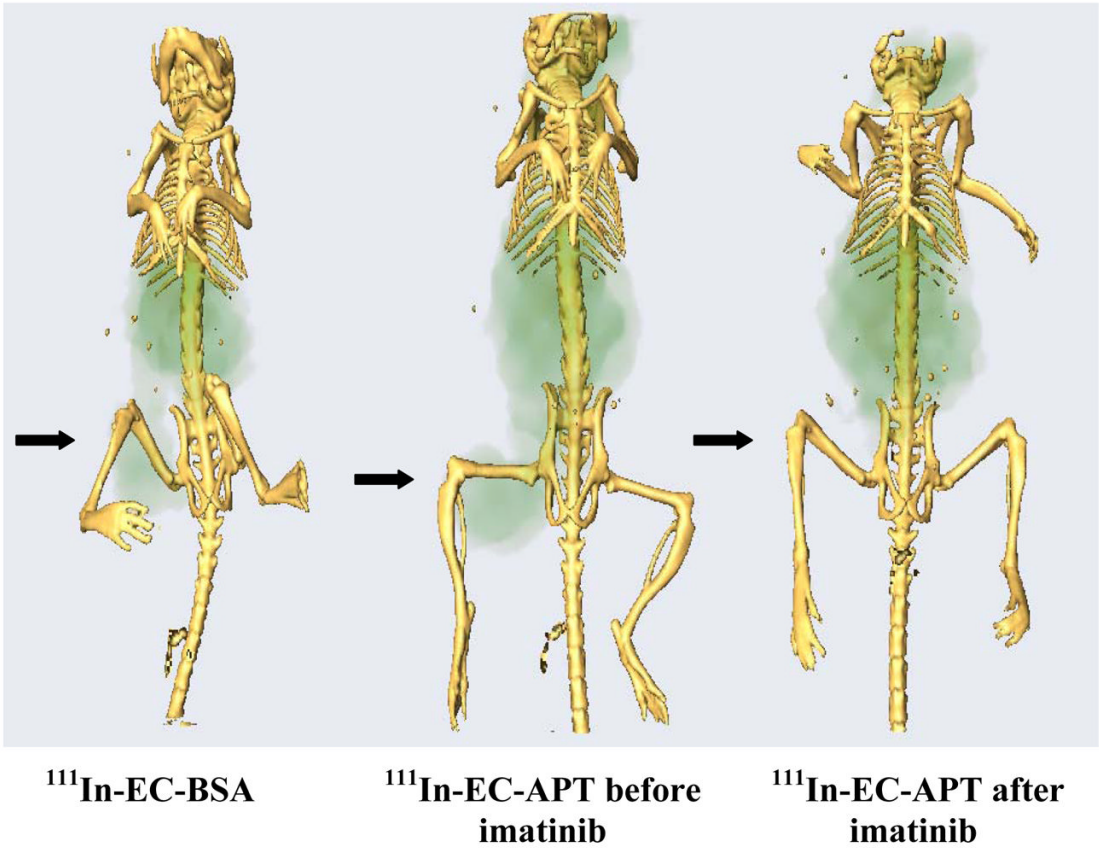

Figure 1.

48 hr iso-surface snap of SPECT-CT images comparing K562 tumor-bearing nude mice injected with ^{111}In-EC-BSA or ^{111}In-EC-APT before and after 5 days of imatinib treatment. Images were fused together using the Amira software, which allows visualization of bony structures in three dimensions. Left panel imaged with ^{111}In-EC-BSA shows baseline levels of blood flow to the tumor (right leg). Middle panel imaged with ^{111}In-EC-APT detects the phosphokinase. Right panel imaged with ^{111}In-EC-APT after 5 days of imatinib shows down-regulation of the phosphokinase. Previous experiments have shown that radiolabeled isotypic control antibody does not image (8).

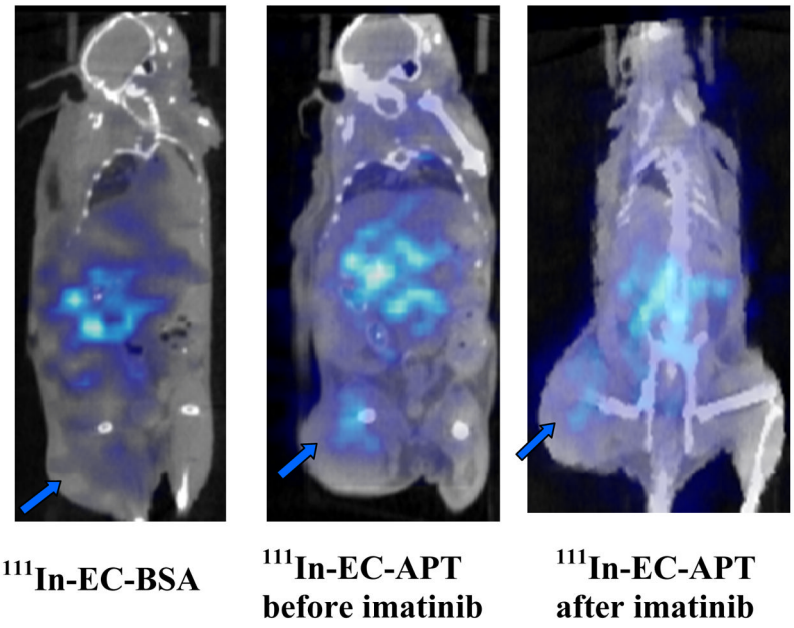

Figure 2.

48 hr comparison of coronal SPECT-CT images of ^{111}In -EC-BSA or ^{111}In -EC-APT injected nude mice before and after 5 day imatinib therapy. Amide software was used for soft tissue analysis. Left panel imaged with ^{111}In-EC-BSA show baseline levels of blood flow to the tumor (right leg). Middle panel imaged with ^{111}In-EC-APT detects the phosphokinase. Right panel imaged with ^{111}In-EC-APT after 5 days of imatinib shows downregulation of phosphokinase.

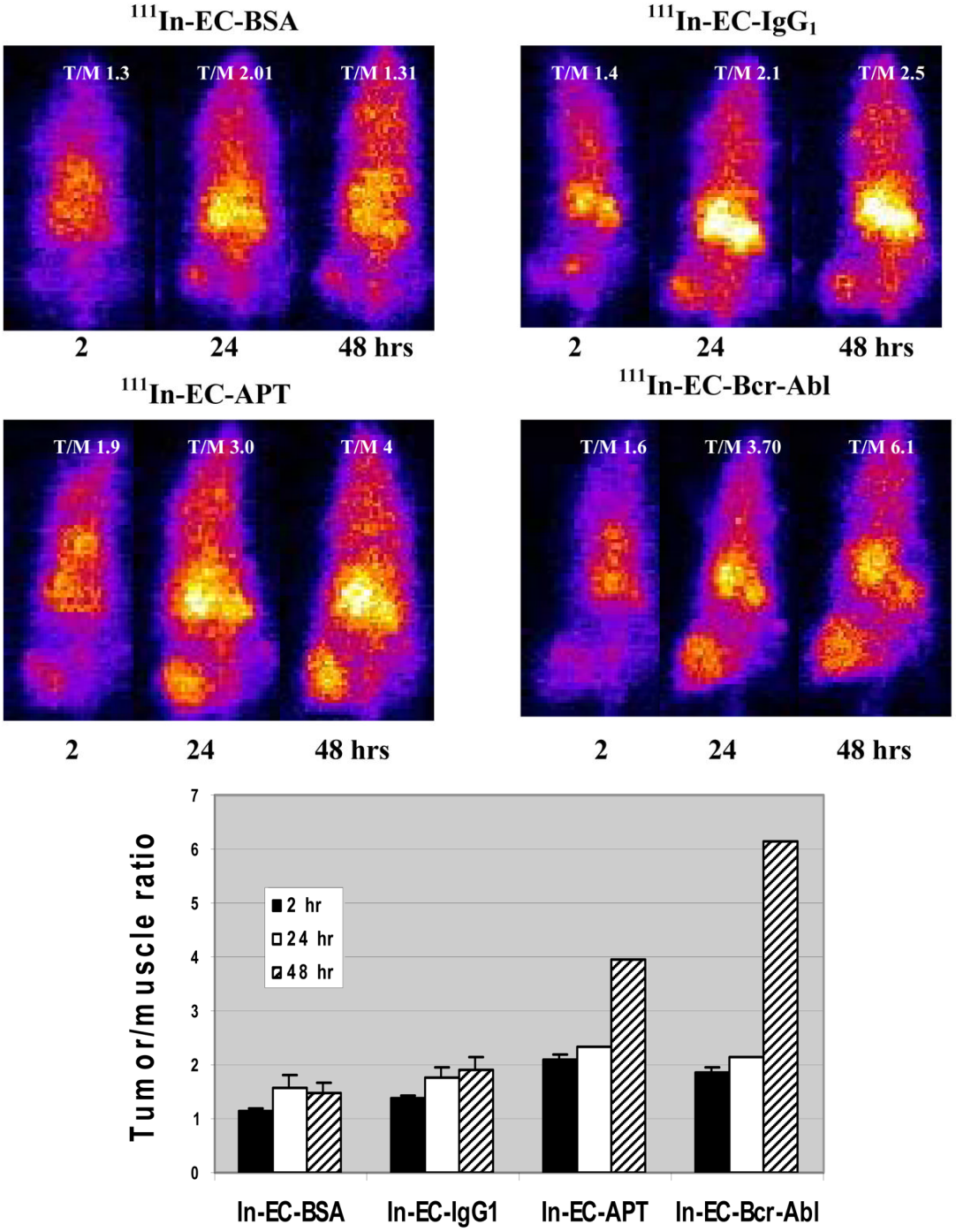

Figure 3.

a) Comparison of uptake of different radio-labeled compounds into K562 xenografts. Planar images of K562 xenografts were taken 2, 24, or 48 hours after injection of ^{111}In-EC-BSA, ^{111}In–EC-IgG$_1$, ^{111}In-EC-APT, or ^{111}In–EC-Bcr-Abl. Scintigraphic images were acquired following radiotracer injection using a gamma camera equipped with a medium energy collimator. b) Average tumor to muscle count density ratios of ^{111}In-EC-BSA, ^{111}In–EC-IgG$_1$, 111In EC-APT, and 111In–EC-Bcr-Abl Regions of interest (counts per pixel) at the tumor lesion site and the symmetrical normal muscle site were used to determine tumor/muscle

count density ratios. Graph shows 2, 24, and 48 hours after injection of ^{111}In-labeled antibodies. Xenografts injected with ^{111}In EC-APT and ^{111}In–EC-Bcr-Abl had higher T/M count density ratios than mice injected with radio-labeled BSA or IgG_1, most notably at 48 hours post-injection.

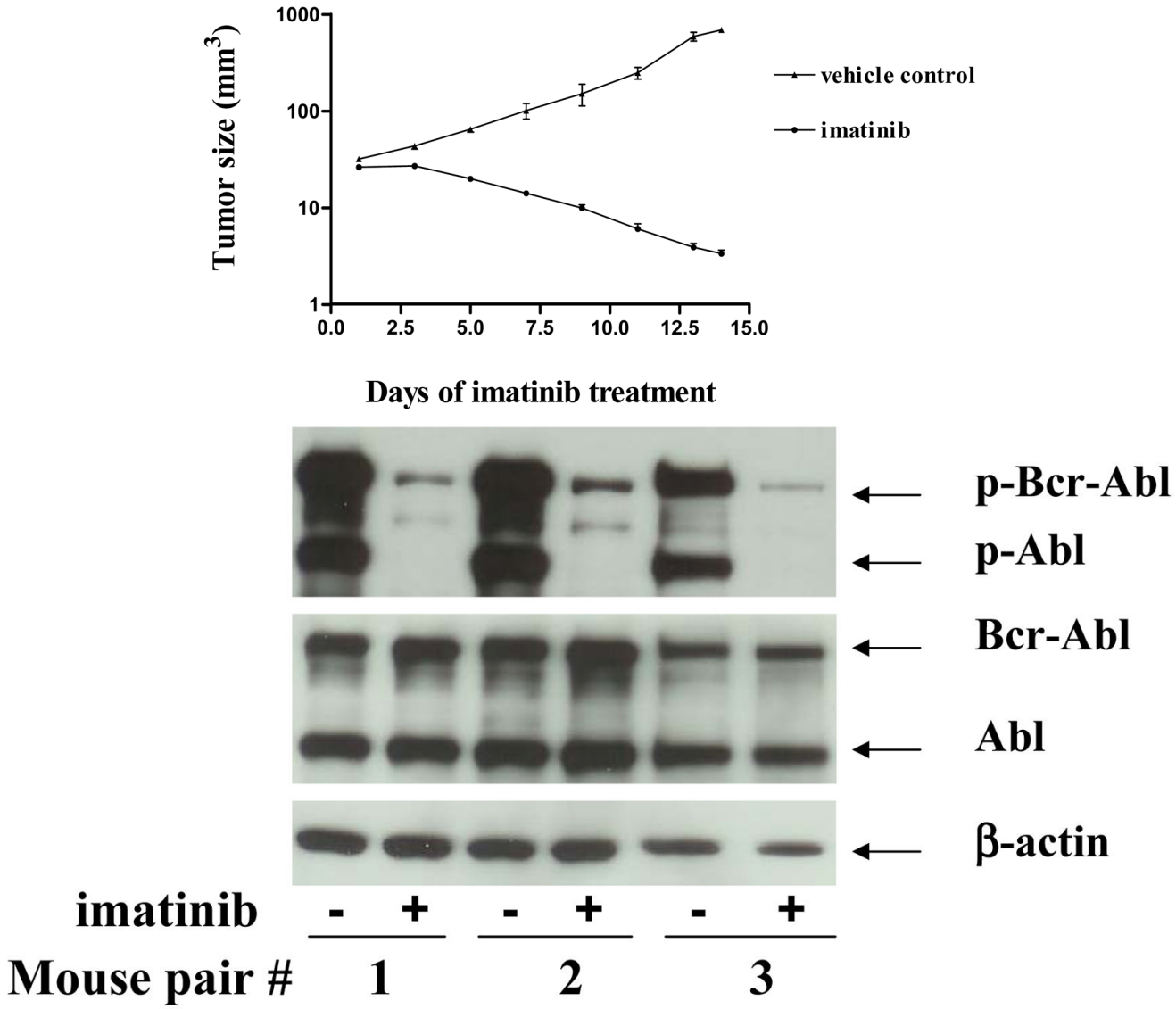

Figure 4.

a) Comparison of tumor volume in K562 xenografts with or without imatinib treatment for 14 days. In the control group, 100 μl of PEG-300 resuspended in sterile water was given by oral gavage daily; imatinib (100mg/kg) was given to the mice in the experimental group in the same manner as the vehicle control was delivered. Both control treated- and imatinib treated-mice started with tumors of about 0.3 cm in diameter. Tumor size was measured every other day until day 14 after treatment. Tumor regression in the imatinib-treated mice is negligible to mild during the first week, but marked by day 14. Tumors grow significantly in the vehicle control treated mice. b) Western blot showing changes in Bcr-Abl and Abl protein phosphorylation in three pairs of K562-bearing xenografts with or without imatinib treatment for 14 days. Anti-β-actin antibody was used as a control for protein loading. Steady-state levels of phosphorylated Bcr-Abl and Abl, but not total Bcr-Abl or Abl are significantly decreased on day 14.

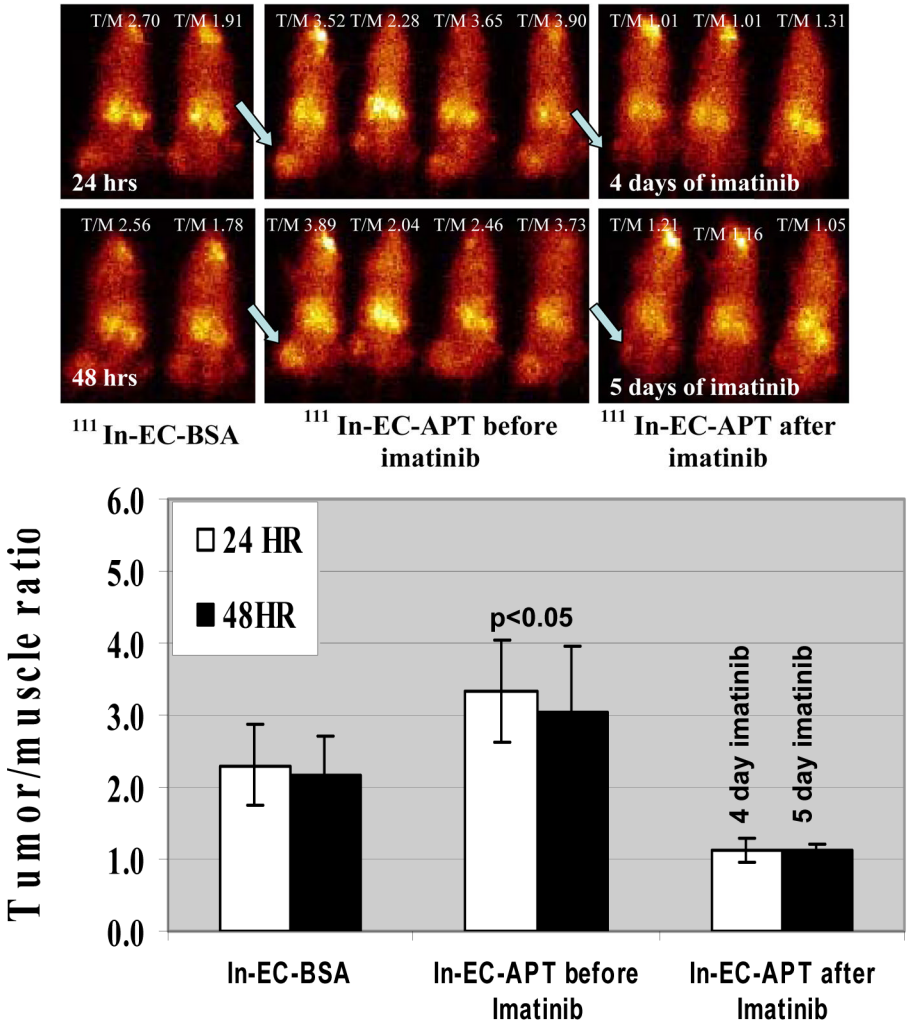

Figure 5.

a) Planar images of K562 xenografts 24 or 48 hours after injection of ^{111}In -EC-BSA or ^{111}In -EC-APT before and after 4 or 5 day imatinib treatment. b) Average tumor to muscle count density ratios of ^{111}In-EC-BSA and ^{111}In EC-APT before and after 4 or 5 day imatinib therapy of K562 xenografts (n = 5 in each group). Data shows 24 and 48 hours after injection of ^{111}In-labeled antibodies. Mice injected with ^{111}In-EC-APT had higher tumor/muscle count density ratios than mice treated with ^{111}In-EC-BSA ($p<0.05$). Furthermore, after treatment with 4 or 5 days of imatinib, respectively, tumor/muscle count density ratios are markedly decreased ($p<0.05$, student's t test).